The human-specific nicotinic receptor subunit CHRFAM7A reduces α7 receptor function in human induced pluripotent stem cells-derived and transgenic mouse neurons

Ilayda Görgülü, Vinita Jagannath, Stéphanie Pons, Filip Koniuszewski, Matthias Groszer, Uwe Maskos, Sigismund Huck, Petra Scholze

Received: 14 December 2023 | Revised: 12 June 2024 | Accepted: 7 July 2024

DOI: 10.1111/ejn.16474

RESEARCH REPORT

EJN European Journal of Neuroscience FENS WILEY

The human-specific nicotinic receptor subunit CHRFAM7A reduces α7 receptor function in human induced pluripotent stem cells-derived and transgenic mouse neurons

Ilayda Görgülü[1] | **Vinita Jagannath**[2,3] | **Stephanie Pons**[4] | **Filip Koniuszewski**[1] | **Matthias Groszer**[2] | **Uwe Maskos**[4] | **Sigismund Huck**[1] | **Petra Scholze**[1]

[1]Center for Brain Research, Medical University of Vienna, Vienna, Austria

[2]Institut du Fer à Moulin, Sorbonne University, UMR-S 1270, Paris, France

[3]MSD R&D Innovation Centre, London, UK

[4]Integrative Neurobiology of Cholinergic Systems, Institut Pasteur, Université Paris Cité, UMR 3571, Paris, France

Correspondence
Petra Scholze, Center for Brain Research, Medical University of Vienna, 1090 Vienna, Austria.
Email: petra.scholze@meduniwien.ac.at

Present address
Vinita Jagannath, Integrative Neurobiology of Cholinergic Systems, Institut Pasteur, Université Paris Cité, UMR 3571, Paris, France.

Funding information
Austrian Science Fund, Grant/Award Number: I3778; Agence Nationale de la Recherche; Fondation de France, Grant/Award Number: 00060522; Fondation Motrice, Grant/Award Number: 2016/4

Edited by: Miriam Melis

Abstract

We investigated the impact of the human-specific gene *CHRFAM7A* on the function of α7 nicotinic acetylcholine receptors (α7 nAChRs) in two different types of neurons: human-induced pluripotent stem cell (hiPSC)-derived cortical neurons, and superior cervical ganglion (SCG) neurons, taken from transgenic mice expressing CHRFAM7A. dupα7, the gene product of *CHRFAM7A*, which lacks a major part of the extracellular N-terminal ligand-binding domain, co-assembles with α7, the gene product of *CHRNA7*. We assessed the receptor function in hiPSC-derived cortical and SCG neurons with Fura-2 calcium imaging and three different α7-specific ligands: PNU282987, choline, and 4BP-TQS. Given the short-lived open state of α7 receptors, we combined the two orthosteric agonists PNU282987 and choline with the type-2 positive allosteric modulator (PAM II) PNU120596. In line with different cellular models used previously, we demonstrate that *CHRFAM7A* has a major impact on nicotinic α7 nAChRs by reducing calcium transients in response to all three agonists.

KEYWORDS
calcium, CHRFAM7A, CHRNA7, hiPSC, nicotinic receptor, superior cervical ganglion

Abbreviations: *CHRNA7*, gene coding for nAChR subunit α7; *CHRFAM7A*, gene fusion between exons 5–10 of *CHRNA7* and *FAM7A*; CHRFAM7A, gene product of *CHRFAM7A*; dupα7, gene product of *CHRFAM7A*; hiPSC, human-induced pluripotent stem cell; nAChR, nicotinic acetylcholine receptor; PAM, positive allosteric modulator; SCG, superior cervical ganglion; α7 nAChR, (pentameric) α7 nicotinic acetylcholine receptor.

1 | INTRODUCTION

The homomeric α7 nAChR is widely expressed in both the brain and periphery with multiple important roles in cognition, memory, and the immune system (reviewed by Bagdas et al., 2018; Bouzat et al., 2018; Ihnatovych et al., 2024; Pastor & Medina, 2023). Decreased expression of *CHRNA7* has been associated with a variety of brain disorders, including schizophrenia, bipolar disorder, attention deficit hyperactivity disorder (ADHD), Alzheimer's disease, autism, epilepsy, and learning disorders (for review, see Ihnatovych et al., 2024; Lew et al., 2018; Sinkus et al., 2015).

It has been reasoned for quite some time that *CHRFAM7A*, a partial duplication of the α7 gene *CHRNA7*, may impair the function of the α7 nAChR (Gault et al., 1998). *CHRNA7* is located at chromosome 15q13.3, an unstable region in the genome, where deletions and gene duplications frequently occur (Gillentine & Schaaf, 2015). *CHRFAM7A* was generated as a fusion product of part of the *CHRNA7* gene with the *ULK4* gene. The protein encoded by this fusion product is called dupα7 and lacks part of the N-terminus of the α7-subunit, including the membrane-trafficking signal peptide and the orthosteric agonist-binding site (Di Lascio et al., 2022; Lang et al., 2014; Sinkus et al., 2015). *CHRFAM7A* is a human-lineage-specific gene that might have first appeared during evolution about 3.5 million years ago (Di Lascio et al., 2022). Like *CHRNA7*, *CHRFAM7A* is widely expressed in the organism (Sinkus et al., 2015).

Decreased expression of *CHRNA7* (Gault et al., 2003) and the presence of *CHRFAM7AΔ2bp* bear an increased risk for schizophrenia (Ihnatovych et al., 2024; Sinkus et al., 2015). Moreover, *CHRNA7* expression and function, possibly regulated by *CHRFAM7A*, may also play a role in inflammation and cancer (reviewed by Di Lascio et al., 2022; Ihnatovych et al., 2024).

dupα7 co-assembles with α7 in a variety of heterologous expression systems (Lasala et al., 2018; Maldifassi et al., 2018; Martin-Sanchez et al., 2021; Wang et al., 2014). Furthermore, if hybrid dupα7/α7 reaches the plasma membrane, the application of α7 agonists may induce currents (Lasala et al., 2018; Wang et al., 2014). However, most reports agree upon that the presence of *CHRFAM7A* significantly attenuates the membrane expression and/or function of α7 nAChRs (Araud et al., 2011; Chan et al., 2019; de Lucas-Cerrillo et al., 2011; Ihnatovych et al., 2019; Maldifassi et al., 2018).

Several mechanisms may account for this impairment, starting from transcriptional regulation to translation, assembly, intracellular processing, membrane targeting and turnover, and receptor gating. Homopentameric α7 nAChRs have five identical agonist binding sites. However, and unlike hetero-oligomeric nAChRs, acetylcholine (ACh) occupancy of only one of five binding sites in α7 produces a maximal response (Andersen et al., 2013), and only two α7 adjacent subunits are required when expressed together with dupα7 in BOSC-23 cells to allow channel opening by ACh (Lasala et al., 2018). This argues against reduced binding sites as a prominent mechanism for CHRFAM7A inhibition of α7 nAChRs.

Several heterologous expression systems have been used to study the impact of *CHRFAM7A* on α7 nAChRs. When co-expressed with *CHRNA7* in *Xenopus laevis* oocytes, *CHRFAM7A* significantly reduced membrane targeting of α7 nAChRs (determined by α-bungarotoxin binding) as well as currents in response to ACh (Araud et al., 2011). Observations with the monoclonal antibody mAb 306, which marks the intracellular loop between transmembrane region 3 (TM3) and TM4, indicate indeed reduced membrane targeting of receptors and not just reduced α-bungarotoxin ligand binding sites (de Lucas-Cerrillo et al., 2011). As expected, expression of CHRFAM7A alone failed to produce any agonist-induced currents in *Xenopus* oocytes (de Lucas-Cerrillo et al., 2011) or Bosc-23 cells (Lasala et al., 2018).

An impaired function of α7 nAChRs by CHRFAM7A was observed in a number of other expression systems, such as PC12 (Chan et al., 2019) and SH-SY5Y cells (Martin-Sanchez et al., 2021). Channel open times in response to the combined application of ACh and the PAM II PNU120596 were significantly shorter in HEK293 cells transfected with *CHRFAM7A* when added to *CHRNA7* cDNA (Ihnatovych et al., 2019; Szigeti et al., 2020). Likewise, channel open times were reduced in medial ganglionic eminence (neuronal) precursor cells derived from human-induced pluripotent stem cells (hiPSCs) when expressing *CHRFAM7A*, along with *CHRNA7* (Ihnatovych et al., 2019). However, *CHRFAM7A* overexpression may also have the opposite effect: In THP1 monocytes, *CHRFAM7A* upregulated *CHRNA7*, which, in turn, led to increased binding of α-bungarotoxin on the cell surface (Costantini et al., 2015).

By taking advantage of the extraordinary Ca^{2+} permeability of α7 nAChRs (Seguela et al., 1993), we investigated α7 receptor properties with Fura-2 Ca^{2+} imaging in the absence and presence of CHRFAM7A in two different model systems: (human) iPSC-derived cortical neurons, and mouse superior cervical ganglion (SCG) neurons. In order to prevent receptor desensitization, we combined the α7 nAChR agonists choline and PNU282987 with the PAM II PNU120596 (Chatzidaki et al., 2015). We also

tested the allosteric agonist 4BP-TQS, which binds to the transmembrane region of α7, does not require the (extracellular) α7 canonical binding site for channel gating, and activates the receptor with minimal desensitization (Chatzidaki et al., 2015). We find that by significantly reducing the Ca^{2+} transients in response to receptor activation, the presence of CHRFAM7A impairs α7 nAChR receptor function in both our model systems.

2 | MATERIALS AND METHODS

2.1 | Animals

Superior cervical ganglia (SCG) were retrieved from four different types of mice: (1) C57Bl/6J (WT, Jackson Laboratory); (2) mice with deletion of the nAChR subunit gene *CHRNA7* (α7 KO) (Orr-Urtreger et al., 1997) (Jackson Laboratory); (3) transgenic mice expressing both *CHRNA7* and *CHRFAM7A* (α7/dupα7); and (4) mice expressing only *CHRFAM7A* (dupα7).

The transgenic mice expressing both *CHRNA7* and *CHRFAM7A* were kindly provided by Andrew Baird, University of California, San Diego (Costantini et al., 2019). By crossing α7/dupα7 male with WT female animals, we bred 50% WT and 50% α7/dupα7 animals.

We then crossed α7/dupα7 mice with α7 KO mice to generate α7 KO/dupα7 mice. Pairing male α7 KO/dupα7 mice with female α7 KO mice results in half and half α7 KO and α7 KO/dupα7 (see crossing protocol; Table S1). The pups were genotyped according to Costantini et al. (2019) and used individually for preparing the SCG cell cultures.

Animals were kept in thermo-stable rooms (21°C) on a light/dark schedule of 10/14 h in group cages with food and water freely accessible. All animal experiments were in accordance with EU (Directive 210/63/EU) and Austrian federal law (Tierversuchsgesetz 2012).

2.2 | Cell cultures of SCG neurons

SCG cultures were prepared as described previously (Fischer et al., 2005). Briefly, SCG were dissected from 4- to 6-day-old (P4 to P6) mouse pups killed by decapitation and collected in Ca^{2+}-free Tyrode's solution (150-mM NaCl, 4-mM KCl, 2-mM $MgCl_2$, 10-mM glucose, 10-mM Hepes, pH 7.4). Ganglia were freed from adhering tissue and incubated in collagenase/dispase for 20 min at 37°C (0.5 mg/mL collagenase IA, Sigma-Aldrich/Merck; 1 mg/mL dispase II, Roche/Merck, in Ca^{2+}-free Tyrode). Subsequently, ganglia were rinsed once with Ca^{2+}-free Tyrode and trypsinized for 15 min at 37°C (0.25% trypsin, Worthington, in Ca^{2+}-free Tyrode). Ganglia were then washed once with Ca^{2+}-free Tyrode and triturated in culture medium, using fire-polished glass Pasteur pipettes.

Dispersed neurons were plated on glass coverslips (13-, 15-, or 25-mm diameter). The coverslips were pretreated with concentrated nitric acid for 2 days, thoroughly rinsed with distilled water, and stored for later use. The coverslips were then coated with 25 μg/mL poly-DL-lysine (Sigma-Aldrich/Merck) overnight at room temperature, followed by 10 μg/mL laminin (Sigma-Aldrich/Merck) dissolved in Neurobasal-A medium (Gibco/Thermo Fisher) overnight at 37°C. The neurons from one single pub were seeded into glass rings of 8-mm diameter to confine the cells to the centre of the coverslips. The tails of the pubs were saved for the follow-up genotyping.

The culture medium consisted of Neurobasal-A medium (Gibco/Thermo Fisher), supplemented with 20 μL/mL B27 (Gibco/Thermo Fisher), 100 U/mL penicillin-100 μg/mL streptomycin (Gibco/Thermo Fisher), 1.5-mM L-glutamine (Sigma-Aldrich/Merck), 20 ng/mL NGF, and 1% foetal calf serum (FCS) (Sigma-Aldrich/Merck). Cultures were maintained at 5% CO_2 at 37°C and used the next day.

2.3 | Human iPSC-derived neuronal cell cultures

The WTS2 hiPSC line is from the Wellcome Trust Sanger Centre collection (https://www.sanger.ac.uk/collaboration/hipsci/, line WTS2). The cell line contains two copies of but does not express *CHRFAM7A*, as verified by RT-PCR and genomic sequence analysis (Llach Pou et al., 2024).

Neural precursor cells (NPC) were generated according to D'Alessio (D'Alessio et al., 2020). The hiPSC-derived cells were then differentiated into neurons. We seeded the thawed NPCs (passages 5–12) onto 60-mm standard polystyrene (PS) cell culture dishes (Sarstedt red colour for adherent cells). Dishes were coated with poly-L-ornithine (PLO) (10 μg/mL) overnight, followed by laminin (10 μg/mL) for 4–16 h. The NPC culture medium contained Advanced DMEM F-12, 1% N2 Supplement, 2% B27 Supplement, 0.01% Penicillin–Streptomycin, 1% GlutaMAX™, 50 mM 2-mercaptoethanol, all Thermo Fisher; 20 ng/μL epidermal growth factor (EGF) (Miltenyi Biotec), and 20 ng/μL fibroblast growth factor (FGF2) (Miltenyi Biotec).

Once the cells reached 100% confluence, they were detached using StemPro™ Accutase™ Cell Dissociation Reagent (Gibco/Thermo Fisher) and either differentiated, expanded further, or cryopreserved at a density of 2–3 × 10^6 cells/mL. Cells were seeded at a density of

10.000/cm^2 either into 35-mm Nunclon Delta cell culture dishes or on PLO/laminin-coated glass coverslips.

For differentiation, the NPC culture medium was changed on the next day to complete BrainPhys Neuronal Medium (StemCell Technologies) containing 1% N2 Supplement A, 2% SM1 Supplement, and the growth factors 20 ng/mL GDNF (Miltenyi Biotec), 20 ng/mL brain-derived neurotrophic factor (BDNF) (Miltenyi Biotec) (Bardy et al., 2015), and 20 ng/mL insulin-like growth factor (IGF1) (Miltenyi Biotec) (Rosa et al., 2020) 0.01% Penicillin–Streptomycin (Thermo Fisher), 0.5-mM dibutyryl cAMP (Sigma Aldrich), 0.2-mM L-ascorbic acid (Sigma Aldrich), 1 µg/mL laminin (Sigma Aldrich), and 1% CultureOne Supplement (Thermo Fisher). After at least 30 days in vitro, cultures were subjected to immunocytochemistry with markers mentioned below, or analysed with either patch clamp electrophysiology or Fura-2 Ca^{2+} imaging.

2.4 | Transduction protocol

NPCs at 70% confluency were seeded on 25-mm glass coverslips placed in 35-mm Nunclon Delta cell culture plastic dishes and infected with PGK-CHRFAM7A-ires-tdTomato lentiviral vector (LV) (MOI 5) or PGK-mCherry LV (100 ng/µL, final concentration) for 24 h. Cultures were then differentiated in complete BrainPhys medium for 30–35 days in the presence of growth factors mentioned above.

2.5 | LV pGK-CHRFAM7A-ires-tdTomato and pGK-mCherry

To create the pLV-PGK-mCherry-WPRE vector, a two-step strategy was used to substitute the eGFP sequence in the pre-existing pTRIP-PGK-eGFP LV (Maskos et al., 2005). First, mCherry cDNA was amplified from the pRSET plasmid (a kind gift of the laboratory of S. Tajbakhsh, Stem Cells and Development lab, Institut Pasteur, Paris, France), using the following primers: forward, 5′-GTACTCGAGCCACCATGGTGAGCAAGGGC-3′; reverse, 5′-GCTGACGCGGCCGCTTACTTGTACA GCTCGTCCATG-3′—and the T/A cloning strategy was used to introduce mCherry cDNA into the pGEM-T Easy vector (Promega). Next, we took advantage of the XhoI restriction site in the multiple-cloning region of the vector to replace the fragment encoding eGFP in the pre-existing pTRIP-PGK-eGFP LV with mCherry cDNA between the XhoI and BsrGI sites.

To create the pLV-PGK-CHRFAM7A-IRES-tdTomato-WPRE vector, we started with the previously described pLV-PGK-α5-IRES-tdTomato-WPRE vector (Koukouli et al., 2017). We excised the part of the sequence coding the α5 nicotinic subunit, and replaced it with by the CHRFAM7A sequence taken from the plasmid pLVx-CHRFAM7A-IRES-ZSGreen (a kind gift from Dr Andrew Baird, Department of Surgery, University of California). Briefly, the fragment containing the CHRFAM7A sequence and part of the IRES sequence were excised with the restriction enzymes XhoI and AvrII, and then this fragment was cloned using the same restriction sites into the pLV-PGK-α5-IRES-tdTomato-WPRE after excision of the α5 subunit.

2.6 | Lentiviral particle generation

Production of lentiviral particles was performed as previously described (Maskos et al., 2005). Briefly, viral particles were generated by co-transfection of HEK-293T cells with the vector plasmid, a packaging plasmid and an envelope plasmid using the calcium phosphate protocol. At 2 days after transfection, viral particles were collected in the supernatant and treated with DNase, passed through a 0.45-µm filter, concentrated by ultracentrifugation, and resuspended in a small volume of PBS. Viral stocks were stored in small aliquots at −80°C before use. Viral titres were estimated by quantification of the p24 capsid protein using the HIV-1 p24 antigen immunoassay (ZeptoMetrix) according to the manufacturer's instructions.

2.7 | Patch-clamp electrophysiology

he electrophysiological recordings for whole-cell patch-clamp were conducted as described (Bardy et al., 2015, 2016; David et al., 2010; Fischer et al., 2005). We used an artificial cerebrospinal fluid (ACSF) solution consisting of: 120-mM NaCl, 3-mM KCl, 2-mM $MgCl_26H_2O$, 2-mM $CaCl_22H_2O$, 20-mM glucose, and 10-mM HEPES. In order to prevent action potentials, tetrodotoxin (TTX) was added as indicated at a final concentration of 1 µM. The Axon Instruments Digidata 1320A 16-bit data acquisition system and Clampex 10.7 software from Molecular Devices were utilized for collecting and analysing data. Patch electrodes were filled with an internal solution consisting of 130-mM K-gluconate, 6-mM KCl, 4-mM NaCl, 10-mM HEPES, 0.2-mM EGTA, 2-mM Mg-ATP, 0.2-mM cAMP, and 10-mM glucose adjusted to pH 7.3 with NaOH.

The internal solution had a pH of 7.3 and an osmolarity ranging from 290 to 310 mOsmol. Patch pipette resistance ranged from 3 to 7 MΩ. All

recordings were carried out at room temperature and low-pass filtered at 2 kHz before digitization and sampling.

We recorded miniature excitatory postsynaptic currents (mEPSCs) in hiPSC-derived neurons in the presence of 1-μM tetrodotoxin (TTX) without and with applications of 2-μM PNU282987 and 10-μM PNU120594 at a holding potential of −70 mV. Detection was triggered by crossing an amplitude threshold set close to the noise for individual neurons (Bellingham et al., 1998). Na^+ and K^+ currents were routinely recorded by depolarizing voltage steps from a holding potential of −80 mV. Cells had an average resting membrane potential of −55 mV. In order to check for action potentials, the membrane potential was raised by current injection to −65 mV, and incremental current steps (2 pA, 500 ms) were applied until trains of action potentials were elicited.

2.8 | Fura-2 Ca^{2+} imaging

Measurements of intracellular Ca^{2+} concentrations were performed at room temperature (22°C–24°C) on an inverted Nikon Diaphot 300 microscope connected to a spectrofluorometrical calcium imaging system (VisiTech, Sunderland, UK). Cells on glass coverslips were incubated for 30 min in culture medium containing 5-μM Fura-2 acetoxymethyl ester (Fura-2 AM, hellobio, Bristol, UK) at 37°C. Uncleaved Fura-2 AM was removed by incubation in culture medium for 20 min at 37°C. The bathing solution was identical to the ACSF solution used for patch clamp recording mentioned above. Changes in intracellular Ca^{2+} concentrations were determined by dual excitation at 340 and 375 nm and emission at 510 nm. Excitation light from a FuraLED Light Source (Cairn Research, Faversham, UK) was directed to the sample via an appropriate filter set. Images were taken with a Nikon Fluor 40×/1.3 Ph4DL oil immersion objective and a Hamamatsu sCMOS ORCA-Flash4.0 Camera. Recording of 340/375 ratio images was at 1 Hz and controlled by VoxCell Workstation and Acquisition Software (VisiTech, Sunderland, UK).

Substances were dissolved in recording buffer and applied in the presence of 1 μm tetrodotoxin (TTX, Latoxan) by a superfusion device (DAD-12, Adams & List). Application times were normally 20 s. After each application, the recording chamber was flushed by an additional superfusion system at a rate of 0.4 mL/min. The effects of drugs were assessed by the increase of ratios from baseline according to Formula 1:

$$E = \frac{Rs - Rb}{Rb}$$

where E is the normalized effect, Rs is the ratio in response to a substance, and Rb is the ratio before the application of a substance.

2.9 | Immunocytochemistry

Cells were seeded onto PLO/laminin-coated 13-mm glass coverslips and fixed with 4% paraformaldehyde at room temperature for 15 min. The samples were then blocked with a blocking buffer (consisting of 3% BSA, 0.3% sodium azide, 1% normal donkey serum, and 0.1% triton X in PBS) at room temperature for 1 h. After blocking, the samples were incubated overnight at 4°C with primary antibodies in a dilution buffer (3% BSA, 0.3% sodium azide, 1% normal donkey serum, and 1% tween 20 in PBS). Subsequently, the samples were incubated with secondary antibodies (488-rabbit and 568-mouse) in dilution buffer at room temperature for 1 h. The samples were then mounted in Prolong Glass Mountant and visualized by fluorescent microscopy.

2.10 | Chemicals

Chemicals were obtained from the following sources: PNU282987 and PNU120596 (Alomone Labs or Tocris), 4BP-TQS and CNQX (6-Cyano-7-nitroquinoxaline-2,-3-dione disodium, Tocris), tetrodotoxin (TTX, Latoxan). All other reagents not mentioned above were obtained from Sigma-Aldrich (Merck, St. Louis, MO).

2.11 | Antibodies

Antibodies were obtained from the following sources (catalogue number and final concentrations in parenthesis): mouse MAP 2 (Sigma M9942, 0.8 μg/mL), rabbit Tuj1 (GeneTex GTX129913, 0.4 μg/mL), rabbit Synapsin I (GeneTex GTX82594, 0.4 μg/mL), mouse tyrosine hydroxylase (TH, Synaptic Systems 213211, 0.4 μg/mL), rabbit vesicular glutamate transporter 1 (vGlut1 Synaptic Systems 135303, 1 μg/mL), mouse NeuN (Millipore MAB377, 1 μg/mL), and rabbit glutamate decarboxylase (GAD65/67 Abbkine Abp51391, 2 μg/mL). All secondary (anti-rabbit 488 and anti-mouse 568) antibodies were from Thermo Fisher Scientific.

2.12 | Analysis and statistics

Analysis of electrophysiology and Ca^{2+} imaging data was conducted using Clampfit 10.7, VoxCell (Visitech), and Excel. The data were rarely normally distributed and thus analysed with nonparametric tests, Mann–Whitney tests when paired, or with Kruskal–Wallis ANOVA, followed by Dunn's multiple comparison test for multiple data sets. One-sample Wilcoxon signed rank tests were applied to check for significant differences from zero. Fura-2 ratios normalized to baseline are shown as median with a 95% confidence interval. GraphPad Prism version 9.4.1 GraphPad Software, San Diego, California, USA (www.graphpad.com) was used for statistical analysis and plotting the graphs (Bardy et al., 2015).

3 | RESULTS

3.1 | hiPSC-derived neurons are mature and express functional α7 receptors

In order to study neuronal physiology, we adopted the protocol by Bardy et al. (2015, 2016) to differentiate hiPSCs into neurons (Figure 1a). In contrast to widely used classical neurobasal media, BrainPhys-media better mimics the in vivo brain environment, which leads to significantly improved neuronal and synaptic activity and survival. After 30 days, cultures formed neuronal networks and expressed the neuronal markers MAP 2 (microtubule-associated protein 2) and TUJ1 (beta-III tubulin) (Figure 1). Overall, about 50% of cells were neurons (TUJ1+/MAP 2+), the rest being glial fibrillary acidic protein (GFAP)-positive astrocytes (Figure 1b6). Our observations are consistent with a previous report (Bardy et al., 2015) that human NPCs differentiated not only into neurons but also into a population of astrocytes staining positively for GFAP.

By using antibodies directed against glutamate decarboxylase 65/67 (GAD65/67), vesicular glutamate transporter (vGLUT), and tyrosine hydroxylase (TH), we identified GABAergic, glutamatergic, and catecholaminergic neurons, respectively (Figure 1b2–b4). Based on our immunostaining, we estimated that 66% are glutamatergic, 25% are GABAergic, and 9% are catecholaminergic cells. Furthermore, some MAP 2-positive cells expressed the cholinergic marker vesicular acetylcholine transporter (vAChT; Figure 1b5).

We then carried out patch-clamp electrophysiology to further characterize the neurons. Four- to 6-week-old hiPSC-derived neurons had an average resting membrane potential of −55 mV. With the membrane potential adjusted to −65 mV, and upon adequate current injection, cells fired a train of action potentials, indicating that they are mature neurons (Figure 1c1) (Bardy et al., 2015). Application of the α7 nAChR ligand PNU282987 when combined with the α7 type-II PAM PNU120596 induced mEPSC activity (Figure 1c3). This activity was prevented in the presence of the AMPA antagonist CNQX (Figure 1c2), indicating the glutamatergic nature of events.

3.2 | CHRFAM7A reduces Ca^{2+} transients in response to α7 ligands in human iPSC-derived neurons

The hiPSC line WTS2 (https://www.sanger.ac.uk/collaboration/hipsci/) contains two copies of *CHRNA7* but no *CHRFAM7A*. This was verified by RT-PCR and genomic sequence analysis (Llach Pou et al., 2024). We transduced cells with a LV (Figure 2a) with or without co-expression of *CHRFAM7A* and recorded Ca^{2+} transients with Fura-2 Ca^{2+} imaging in response to α7 nAChR activation (Figure 2). Lentivirus without a specific neuronal promoter transduced both neurons and nonneuronal cells. Approximately 40% per cent of the cells were transduced with *CHRFAM7A*-tdTomato LV (Figure 2b1), and similar results were obtained with mCherry LV without *CHRFAM7A* (Figure 2b2). As shown in Figure 2d, α7 nAChR ligands generated significantly smaller responses in hiPSC-derived neurons transduced with *CHRFAM7A*-tdTomato than in nontransduced (non-fluorescent) neurons. As viral infection of cells per se reduces Ca^{2+} responses (data not shown), we compared the effect of α7 nAChR activation in neurons transduced with *CHRFAM7A*-tdTomato with effects in mCherry sham-transduced neurons (Figure 2e1–e4).

As shown in Figure 2e1, combined applications of the nAChR agonists PNU282987 and the PAM II PNU120596 caused a large increase of intracellular Ca^{2+} in cells lacking *CHRFAM7A*. PNU120596 prevents desensitization of the receptor and thus the decline of responses at supramaximal concentrations (beyond 1 μM; Larsen et al., 2019). Responses by combined applications of the α7 nAChR agonists PNU282987 and the PAM II PNU120596 in cells infected with LV carrying *CHRFAM7A* were only 6% of responses observed in cells infected with just LV. When applied without the PAM, PNU282987 did not induce any Ca^{2+} transients (not shown).

Likewise, choline alone did not induce measurable responses in hiPSC-derived neurons with or without CHRFAM7A (Figure 2e3). When combined with PNU120596, choline caused large responses in sham-

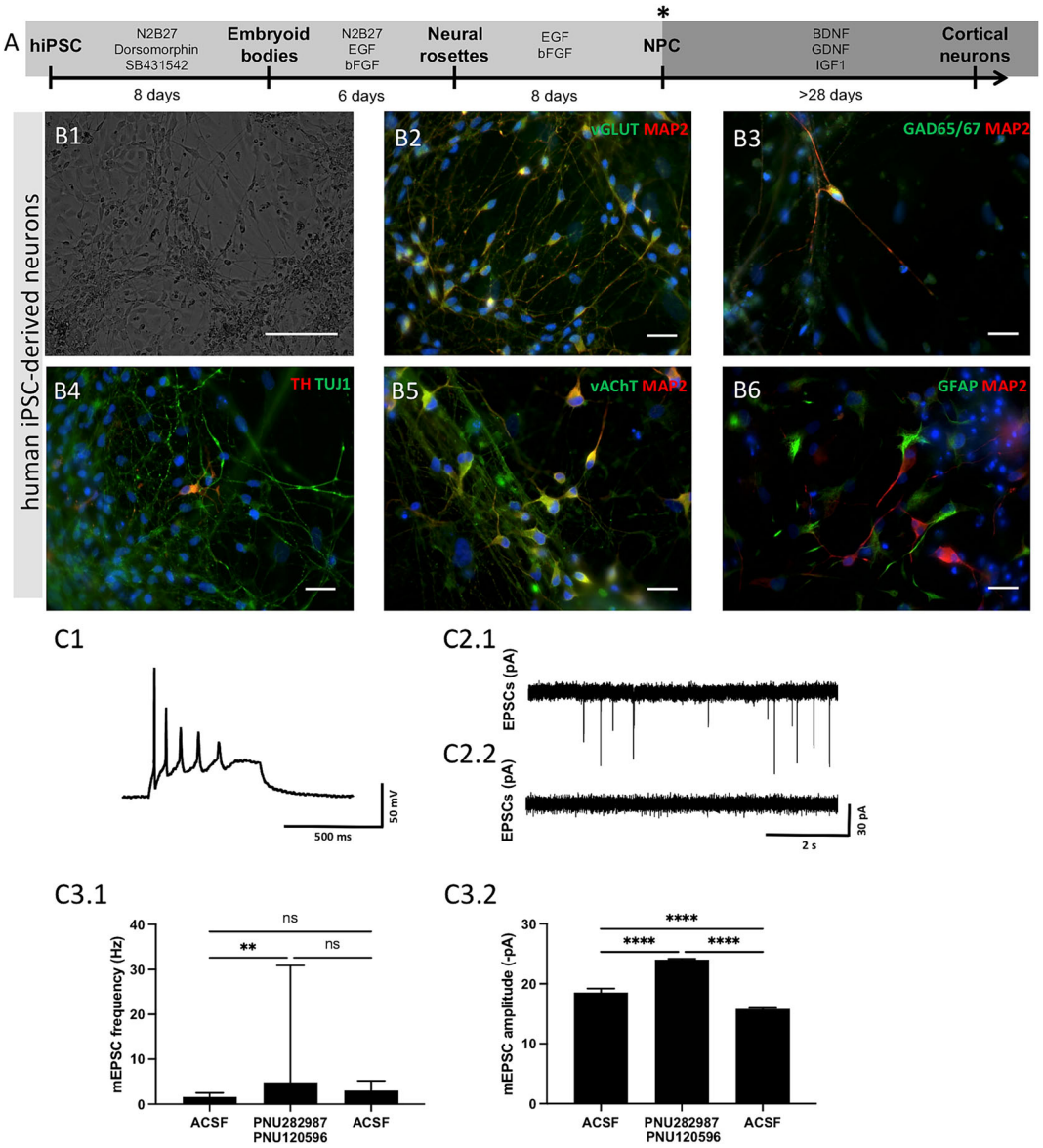

FIGURE 1 Molecular and functional characterization of hiPSC-derived neurons. (a) hiPSC differentiation protocol. Note that transduction with LV (if performed) was done when the status of neuronal precursor cells (NPC) was reached (*). (b1) Bright field image of hiPSC-derived neurons after 32 days of differentiation. (b2–b5) Immunofluorescence staining of hiPSC-derived neurons showing expression of the neuronal markers microtubule-associated protein 2 (MAP 2), beta-III tubulin (TUJ1), tyrosine hydroxylase (TH), vesicular glutamate transporter 1 (vGlut1), and glutamate decarboxylase 65/67 (GAD65/67), as well as the glial marker glial fibrillary acidic protein (GFAP) (b6). Cells were differentiated for 30–40 days. Scale bars: 150 μm (B1); 20 μM (B2-B6). (c1) Current clamp recording of a cell after 35 days of differentiation. Current injection (6 pA, 500 ms) from holding potential (−65 mV) induced a train of action potentials Scale bars: 50 mV, 0.5 s. (c2.1) Miniature excitatory postsynaptic currents (mEPSCs) without and (c2.2) with application of 10 μM of the AMPA antagonist CNQX. Scale bar: 30 pA, 2 s. Graphs in panel c3.1 show mEPSCs frequency, and panel c3.2 shows amplitudes from 24 cells, obtained from four different NPC cultures differentiated for at least 30 days. Events were counted 30 s before, during 30-s application, and 30 s after application of 2-μM PNU120596, combined with 10 μM PNU120596 in the presence of 1-μM tetrodotoxin (TTX). Counts were then divided by 30 to obtain the frequency (Hz). Note that mEPSC frequency varied significantly between individual cells, even of the same culture. Data are medians with 95% confidence intervals (Kruskal–Wallis, Dunn's multiple comparison test). ns, not significant; $p > 0.05$; **$p < 0.001$; ****$p < 0.0001$.

transduced neurons, whereas this response was reduced by 94% upon expression of *CHRFAM7A* (Figure 2e4).

We next tested the allosteric agonist 4BP-TQS. 4BP-TQS binds to the transmembrane region of α7 (Gill et al., 2011) and does not require the (extracellular) α7

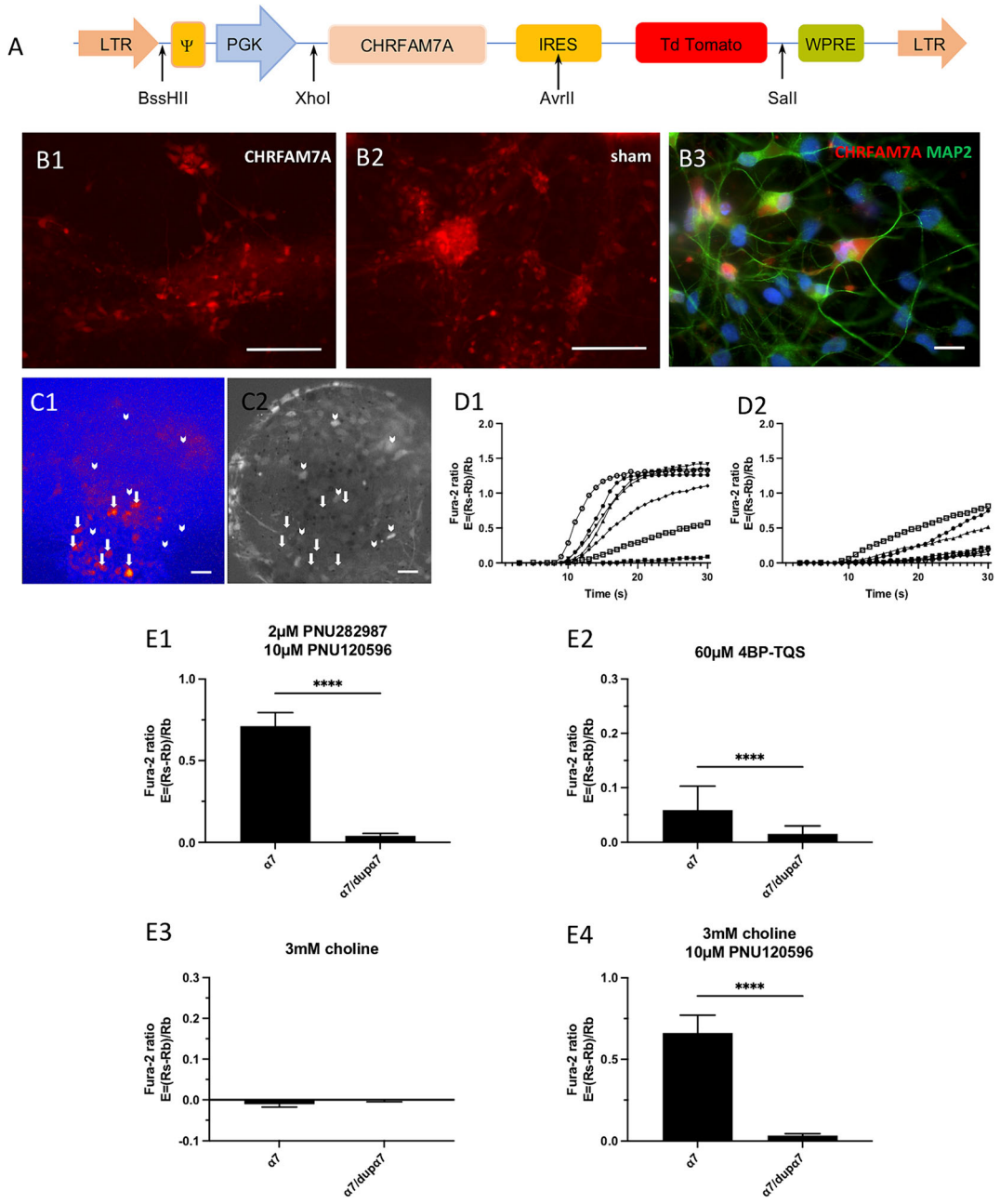

FIGURE 2 Legend on next page.

canonical binding site for channel gating (this part is missing in CHRFAM7A; see Figure S1). 4BP-TQS induced small responses in sham-transduced cells, and these responses were further reduced by 73% in neurons carrying the *CHRFAM7A* gene (Figure 2e2). Similar to previous observations in hiPSC-derived neurons (Chatzidaki et al., 2015), the efficacy of 4BP-TQS is significantly smaller than the efficacy of combined applications of PNU282987 and PNU120596 (compare effects for α7 in Figure 2, panels e1 and e2).

3.3 | CHRFAM7A reduces Ca^{2+} transients in response to α7 ligands in mouse SCG neurons

We then used transgenic mice expressing CHRFAM7A in addition to (mouse) α7 (Costantini et al., 2019). We crossed these mice with WT mice and mice with deletion of the α7 subunit (Orr-Urtreger et al., 1997) to obtain four different types of mice (see Section 2): (1) C57Bl/6 (WT, Jackson Laboratory); (2) mice with deletion of the

FIGURE 2 Expression of *CHRFAM7A* inhibits function of α7 receptors in hiPSC-derived neurons. (a) Lentiviral construct encoding CHRFAM7A and tdTomato. (b1) hiPSC-derived neurons transduced with CHRFAM7 (PGK-CHRFAM7A-ires-tdTomato) or without (b2) CHRFAM7A (mCherry in red fluorescence). Scale bars B1, B2: 150 μm. (b3) CHRFAM7-positive cells express MAP 2. Scale bar: 10 μM. (c1) CHRFAM7A-transduced cell culture. Arrows point at cells transduced with PGK-CHRFAM7A-ires-tdTomato, arrowheads at non-transduced cells. (c2) Same culture as c1: Fura-2 340/375 ratio image upon application of 2-μM PNU282987 plus 10-μM PNU120596. Substances were applied for 15 s, starting at 10 s. Scale bars c1, c2: 150 μm. (d1) Calcium transients shown with Fura-2 calcium imaging in nontransduced and (d2) transduced cells shown in panels c1 and c2 (nontransduced cells: arrowheads; transduced cells: arrows). Responses by individual cells are shown by different symbols. (e1) Effect of 2-μM PNU282987 plus 10-μM PNU120596 in sham-transduced neurons (mCherry-expression, labelled α7) and in *CHRFAM7A*-lentivirus infected neurons expressing both *CHRNA7* and *CHRFAM7A* (labelled α7/dupα7). The effect of the substances is significantly reduced by 94% in cells transduced with *CHRFAM7A* (two-tailed Mann–Whitney test, $p < 0.0001$). (e2) Effect of 60-μM 4BP-TQS in sham-transduced neurons (mCherry-expression, labelled α7) and in *CHRFAM7A*-lentivirus infected neurons expressing both *CHRNA7* and *CHRFAM7A* (labelled α7/dupα7). The effect of 4BP-TQS is significantly reduced by 73% in cells transduced with *CHRFAM7A* (two-tailed Mann–Whitney test, $p < 0.0001$). (e3) Lack of effects of 3-mM choline: No increase was observed in sham-transduced neurons (mCherry-expression, labelled α7) nor in *CHRFAM7A*-lentivirus infected neurons expressing both *CHRNA7* and *CHRFAM7A* (labelled α7/dupα7) (one sample Wilcoxon signed rank test, values not significantly different from zero, $p > 0.05$). (e4) Effect of 3-mM choline in combination with 10-μM PNU120596 in sham-transduced neurons (mCherry-expression, labelled α7) and in *CHRFAM7A*-lentivirus infected neurons expressing both *CHRNA7* and *CHRFAM7A* (labelled α7/dupα7). The effect of the substances is reduced by 94% in cells transduced with *CHRFAM7A* (two-tailed Mann–Whitney test, $p < 0.0001$). Fura-2 calcium imaging was performed in the presence of 1-μM TTX. Fura-2 ratios normalized to baseline are shown as median with 95% confidence interval. Data are the results of at least 130 cells from three batches of differentiated cells. $^{****}p < 0.0001$.

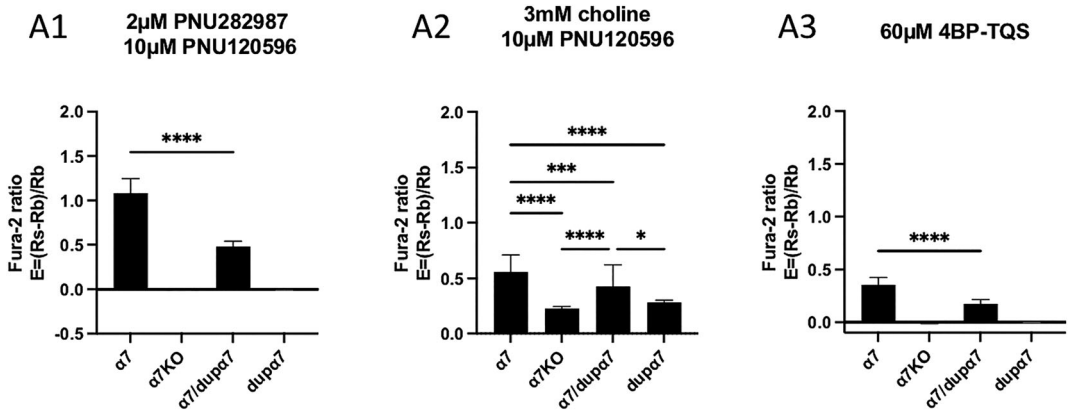

FIGURE 3 Expression of *CHRFAM7A* reduces function of α7 receptors in mouse SCG neurons. Effects of nAChR ligands on SCG neurons taken from C57Bl/6J control mice (α7), from α7 knockout mice (α7 KO), from mice expressing both α7 and dupα7 (α7/dupα7), and from mice expressing just dupα7 (dupα7). (a1) Effects of 2 μM PNU282987 plus 10-μM PNU120596. The effects are significantly reduced by 55% in neurons co-expressing dupα7 (two-tailed Mann–Whitney test, $p < 0.0001$). A small but significant decrease (0.01) of Ca^{2+} was observed in either α7 KO or (just) dupα7 expressing neurons (one sample Wilcoxon signed rank test, significantly different from zero, $p < 0.0001$). (a2) Effects of 3-mM choline plus 10-μM PNU120596. The effects are significantly reduced (by 23%) when neurons co-express dupα7 (Kruskal–Wallis, Dunn's multiple comparison test, $p < 0.0005$). The clear effects on neurons taken from α7 KO mice or mice expressing just dupα7 are due to the low efficacy of choline at α3β4* receptors; (a3) 60-μM applications of the allosteric agonist 4BP-TQS induces calcium transients in SCG neurons taken from C57Bl/6J control mice, but not in neurons taken from α7 KO mice or mice expressing just dupα7. In the presence of dupa7, the response to 4BP-TQS is significantly reduced (by 50%, two-tailed Mann–Whitney test, $p < 0.0001$). Fura-2 calcium imaging was performed in the presence of 1-μM tetrodotoxin (TTX). Fura-2 ratios normalized to baseline are shown as median with 95% confidence interval. Data range from 31 to 228 (mean: 105) cells, collected from three different experiments. $^{****}p < 0.0001$.

nAChR subunit gene *CHRNA7* (α7 KO); (3) transgenic mice expressing both *CHRNA7* and *CHRFAM7A* (α7/dupα7); and (4) mice expressing only *CHRFAM7A* (dupα7).

As illustrated in Figure 3a1, the presence of CHRFAM7A reduced the effect of applications of PNU282987 (combined with PNU120596) by 55%, compared with neurons expressing only α7. SCG neurons from either α7 knockout (KO) animals or animals expressing just CHRFAM7A did not show any response (Figure 3a1). Likewise, the effects of the allosteric agonist 4BP-TQS were significantly smaller (by 50%) in neurons

expressing CHRFAM7A, in addition to α7 (Figure 3a3). 4BP-TQS did not induce any Ca^{2+} increase in neurons from α7 KO animals or neurons obtained from animals expressing just CHRFAM7A (Figure 3a3). Similar to our observations in hiPSC-derived neurons, responses by 4BP-TQS were significantly smaller than responses by combined applications of PNU282987 and PNU120596 (compare α7 in Figure 3a1 and a3).

Along these lines, the combined application of choline with PNU120596 induced a large increase of intracellular Ca^{2+} in control (α7) C57Bl/6 mice, and this increase was significantly attenuated (by 23%) in SCG neurons expressing *CHRFAM7A* in addition to *CHRNA7* (Figure 3a2). However, the application of choline (combined with PNU120596) also triggered effects in neurons taken from α7 KO or CHRFAM7A mice (Figure 3a2). Such choline effects have been observed previously and are due to the activation of α3β4* receptors (see discussion).

4 | DISCUSSION

The α7 nicotinic ACh receptors have important functions in health and disease. Neuronal α7 nAChRs in the brain contribute to cognition, sensory processing, attention, working memory, and reward pathways (reviewed by Bouzat et al., 2018). Impairment of α7 receptor function in neurons has thus been linked to diseases like Morbus Alzheimer and schizophrenia (reviewed by Koukouli & Maskos, 2015). However, α7 receptors are also expressed in nonneuronal cells, both within and outside the brain, thereby affecting peripheral (reviewed by Maldifassi et al., 2018) and central inflammation (as contributing factor to neurodegenerative/demyelinating diseases, reviewed by Piovesana et al., 2021).

Early reports on cloning and expression revealed some exceptional properties of α7 receptors, distinguishing them from hetero-pentameric neuronal nAChRs: Hence, α7 receptors are homo-pentamers, show exceptional Ca^{2+} permeability, and bind—and are potently inhibited by—α-bungarotoxin (Seguela et al., 1993). However, it took some more years to show that α7 may co-assemble with other subunits, for example, β2, to form hetero-pentamers (reviewed by Wu et al., 2016). α7β2 receptors are enriched, for example, in the basal forebrain, a crucial structure for cognition. Loss of α7β2 receptors goes along with cognitive decline (reviewed by Ballinger et al., 2016). Like α7 homo-pentamers, α7β2 hetero-pentameric receptors are inhibited by α-bungarotoxin but differ in their properties by their significantly increased sensitivity to amyloid β peptide (George et al., 2021; Wu et al., 2016). Though of interest, we are not aware of reports on a potential impact of CHRFAM7A on the expression and/or function of α7β2 receptors.

The α7 receptors differ from hetero-pentameric α4β2* and α3β2* receptors by their extremely short-lived open state. Hence, the application of agonists may generate responses that are too low for a proper quantification (Lasala et al., 2018). Because we neither saw clear currents nor intracellular Ca^{2+} increase when we applied just PNU282987 to hiPSC-derived neurons, we combined the agonist with the PAM PNU120596. For judging the impact of CHRFAM7A, experiments were thus generally done in the presence of PNU120596.

The hiPSC line WTS2 offers the opportunity to study the function of α7 receptors in hiPSC-derived neurons in the absence of CHRFAM7A. Upon viral transduction with *CHRFAM7A*, intracellular Ca^{2+} transients measured with Fura-2 were significantly inhibited compared with control cells, transduced with just LV. These results were similar not only upon applications of the orthosteric α7 agonists PNU282987 and choline but also with the allosteric agonist 4BP-TQS. Of interest, 4BP-TQS activates the receptor by binding to the transmembrane domain of the subunit (Gill et al., 2011) (see Figure S1). Hence, reduced orthosteric binding sites due to the presence of the truncated dupα7 subunit cannot fully explain the reduced function of the receptor.

As a complementary approach, we investigated the function of α7 receptors in the absence and presence of CHRFAM7A in mouse SCG neurons. Though α7 receptors are expressed in the superior cervical ganglion (Seddik et al., 2003), they do not serve synaptic transmission in the ganglion (Brown & Fumagalli, 1977; Simeone et al., 2019). Similar to hiPSC-derived neurons, the presence of CHRFAM7A in SCG neurons significantly inhibited Ca^{2+} transients upon applications of the allosteric agonist 4BP-TQS or the orthosteric α7 agonists PNU282987 and choline. Choline with (Figure 3) or without PNU120596 (not shown) induced clear Ca^{2+} transients in both α7 KO mice and in mice expressing just CHRFAM7A. We and others (David et al., 2010; Seddik et al., 2003) reported previously that choline also activates α3β4* receptors and is thus not selective for α7 receptors. As an incidental finding, we did not observe any increase of intracellular Ca^{2+} in response to choline in our hiPSC-derived neurons, suggesting that α3β4* receptors are not expressed to a significant extent. These observations are in line with a previous report that only a low proportion of hiPSC-derived neurons express functional non-α7 nACh receptors (Chatzidaki et al., 2015).

Significant reductions of Ca^{2+} transients (determined with Fura-2) in response to the combined application of PNU282987 plus PNU120596 have recently been

observed in SH-SY5Y cells stably transfected with a dupα7-pcDNA3.1/Myc-His construct (Martin-Sanchez et al., 2021). The impaired function of *CHRNA7* by the presence of *CHRFAM7A* is paralleled by reduced vesicular exocytosis, measured by de-staining of preloaded FM1-43. Most elegantly, removal of endogenous *CHRFAM7A* expression by siRNA significantly enhanced the release of dopamine, endogenous in SH-SY5Y (Martin-Sanchez et al., 2021).

As briefly summarized in Section 1, impaired function of α7 by CHRFAM7A may be explained by several mechanisms, including intracellular processing. It is thus of interest that in hiPSCs and neural progenitor cells (NPCs) derived from individuals with either heterozygous 15q13.3 deletions or heterozygous 15q13.3 duplications, *CHRNA7* copy number variations in both directions reduced α7 nAChR-associated calcium flux. This is likely a consequence of inefficient chaperoning, with accumulation of α7 subunits in the ER, preventing functional α7 nAChRs being incorporated in the cell membrane (Gillentine et al., 2017). A recent report using medial ganglionic progenitors differentiated from UB068 (null) and UB068_CHRFAM7A suggests that CHRFAM7A modifies Ca^{2+} dynamics, with downstream effects on Rac1 and actin cytoskeleton (Szigeti et al., 2023). Though ionotropic mechanisms may be the prevalent function, nicotinic receptors also signal by alternative pathways (Kabbani et al., 2013). Hence, α7 affects nuclear factor κ-B (NF-κB) and Jak2/STAT3 inflammatory (de Jonge et al., 2005) as well as $G\alpha_q$-phospholipase C-IP_3 signalling pathways (King et al., 2015; Zhong et al., 2013). Hence, any interference of CHRFAM7A with α7 expression and/or function would significantly affect responses of the immune system, as well as sustained Ca^{2+} elevations in neurons (King et al., 2015; Zhong et al., 2013). In iPSC-derived microglia-like cells, CHRFAM7A modified the dynamics of NF-κB translocation by prolonging its nuclear presence (Ihnatovych et al., 2020). Expression of CHRFAM7A is particularly high in human bone marrow and circulating $CD14^+$ monocytes (Costantini et al., 2019), crucial components of the immune system. By using RAW264.7 macrophages as a model system, Maldifassi et al. (2018) could thus show with immunoprecipitation and FRET data that dupα7 co-assembles with α7 into mixed dupα7/α7-nAChRs and that *CHRFAM7A* overexpression prevents the anti-inflammatory effect of nicotine in LPS-stimulated RAW264.7 macrophages (Maldifassi et al., 2018).

In conclusion, we demonstrate with Fura-2 Ca^{++} imaging that the human-specific *CHRFAM7A* gene inhibits α7 nAChRs in hiPSC-derived (cortical) neurons. We could, in addition, show similar inhibitory effects in primary mouse SCG neurons. α7 nAChR agonists in the presence of the PAM II PNU120596 did not induce any effect in mouse SCG neurons expressing only *CHRFAM7A*, but not *CHRNA7*.

AUTHOR CONTRIBUTIONS

Ilayda Görgülü, Sigismund Huck, and Petra Scholze wrote the manuscript; Ilayda Görgülü, Matthias Groszer, Uwe Maskos, Sigismund Huck, Petra Scholze, and Stephanie Pons designed the experiments; Ilayda Görgülü and Filip Koniuszewski performed the experiments; Petra Scholze prepared the primary cell cultures from transgenic mice; Vinita Jagannath developed and established the iPSC differentiation protocols.

ACKNOWLEDGEMENTS

This study was supported by the Austrian Science Fund (FWF) grant I 3778, which is part of the ERANET programme "iPS&Brain", coordinated by U.M., who was funded through the French Agence Nationale de la Recherche (ANR). M.G. gratefully acknowledges financial support from the Fondation de France (Eng° 00060522) and the Fondation Motrice (N° 2016/4) and thanks Cedric Bardy for advice on BrainPhys medium. For the purpose of open access, the author has applied a CC BY public copyright licence to any Author Accepted Manuscript version arising from this submission.

CONFLICT OF INTEREST STATEMENT

The authors declare that the research was conducted in the absence of any commercial or financial relationships that could be construed as a potential conflict of interest.

PEER REVIEW

The peer review history for this article is available at https://www.webofscience.com/api/gateway/wos/peer-review/10.1111/ejn.16474.

DATA AVAILABILITY STATEMENT

The original experimental data are available at: https://doi.org/10.5281/zenodo.11184945.

ORCID

Vinita Jagannath https://orcid.org/0000-0001-6785-8181
Petra Scholze https://orcid.org/0000-0003-4984-6034

REFERENCES

Andersen, N., Corradi, J., Sine, S. M., & Bouzat, C. (2013). Stoichiometry for activation of neuronal alpha7 nicotinic receptors. *Proceedings of the National Academy of Sciences of the United States of America*, *110*, 20819–20824. https://doi.org/10.1073/pnas.1315775110

Araud, T., Graw, S., Berger, R., Lee, M., Neveu, E., Bertrand, D., & Leonard, S. (2011). The chimeric gene CHRFAM7A, a partial

duplication of the CHRNA7 gene, is a dominant negative regulator of alpha7*nAChR function. *Biochemical Pharmacology*, *82*, 904–914. https://doi.org/10.1016/j.bcp.2011.06.018

Bagdas, D., Gurun, M. S., Flood, P., Papke, R. L., & Damaj, M. I. (2018). New insights on neuronal nicotinic acetylcholine receptors as targets for pain and inflammation: A focus on alpha7 nAChRs. *Current Neuropharmacology*, *16*, 415–425. https://doi.org/10.2174/1570159X15666170818102108

Ballinger, E. C., Ananth, M., Talmage, D. A., & Role, L. W. (2016). Basal forebrain cholinergic circuits and signaling in cognition and cognitive decline. *Neuron*, *91*, 1199–1218. https://doi.org/10.1016/j.neuron.2016.09.006

Bardy, C., van den Hurk, M., Eames, T., Marchand, C., Hernandez, R. V., Kellogg, M., Gorris, M., Galet, B., Palomares, V., Brown, J., Bang, A. G., Mertens, J., Bohnke, L., Boyer, L., Simon, S., & Gage, F. H. (2015). Neuronal medium that supports basic synaptic functions and activity of human neurons in vitro. *Proceedings of the National Academy of Sciences of the United States of America*, *112*, E2725–E2734. https://doi.org/10.1073/pnas.1504393112

Bardy, C., van den Hurk, M., Kakaradov, B., Erwin, J. A., Jaeger, B. N., Hernandez, R. V., Eames, T., Paucar, A. A., Gorris, M., Marchand, C., Jappelli, R., Barron, J., Bryant, A. K., Kellogg, M., Lasken, R. S., Rutten, B. P., Steinbusch, H. W., Yeo, G. W., & Gage, F. H. (2016). Predicting the functional states of human iPSC-derived neurons with single-cell RNA-seq and electrophysiology. *Molecular Psychiatry*, *21*, 1573–1588. https://doi.org/10.1038/mp.2016.158

Bellingham, M. C., Lim, R., & Walmsley, B. (1998). Developmental changes in EPSC quantal size and quantal content at a central glutamatergic synapse in rat. *The Journal of Physiology*, *511*(Pt 3), 861–869. https://doi.org/10.1111/j.1469-7793.1998.861bg.x

Bouzat, C., Lasala, M., Nielsen, B. E., Corradi, J., & Esandi, M. D. C. (2018). Molecular function of alpha7 nicotinic receptors as drug targets. *The Journal of Physiology*, *596*, 1847–1861. https://doi.org/10.1113/JP275101

Brown, D. A., & Fumagalli, L. (1977). Dissociation of bungarotoxin binding and receptor block in the rat superior cervical ganglion. *Brain Research*, *129*, 165–168. https://doi.org/10.1016/0006-8993(77)90981-7

Chan, T., Williams, E., Cohen, O., Eliceiri, B. P., Baird, A., & Costantini, T. W. (2019). CHRFAM7A alters binding to the neuronal alpha-7 nicotinic acetylcholine receptor. *Neuroscience Letters*, *690*, 126–131. https://doi.org/10.1016/j.neulet.2018.10.010

Chatzidaki, A., Fouillet, A., Li, J., Dage, J., Millar, N. S., Sher, E., & Ursu, D. (2015). Pharmacological characterisation of nicotinic acetylcholine receptors expressed in human iPSC-derived neurons. *PLoS ONE*, *10*, e0125116. https://doi.org/10.1371/journal.pone.0125116

Costantini, T. W., Chan, T. W., Cohen, O., Langness, S., Treadwell, S., Williams, E., Eliceiri, B. P., & Baird, A. (2019). Uniquely human CHRFAM7A gene increases the hematopoietic stem cell reservoir in mice and amplifies their inflammatory response. *Proceedings of the National Academy of Sciences of the United States of America*, *116*, 7932–7940. https://doi.org/10.1073/pnas.1821853116

Costantini, T. W., Dang, X., Yurchyshyna, M. V., Coimbra, R., Eliceiri, B. P., & Baird, A. (2015). A human-specific alpha7-nicotinic acetylcholine receptor gene in human leukocytes: Identification, regulation and the consequences of CHRFAM7A expression. *Molecular Medicine*, *21*, 323–336. https://doi.org/10.2119/molmed.2015.00018

D'Alessio, R., Koukouli, F., Blanchard, S., Catteau, J., Rais, C., Lemonnier, T., Feraud, O., Bennaceur-Griscelli, A., Groszer, M., & Maskos, U. (2020). Long-term development of human iPSC-derived pyramidal neurons quantified after transplantation into the neonatal mouse cortex. *Developmental Biology*, *461*, 86–95. https://doi.org/10.1016/j.ydbio.2020.01.009

David, R., Ciuraszkiewicz, A., Simeone, X., Orr-Urtreger, A., Papke, R. L., McIntosh, J. M., Huck, S., & Scholze, P. (2010). Biochemical and functional properties of distinct nicotinic acetylcholine receptors in the superior cervical ganglion of mice with targeted deletions of nAChR subunit genes. *The European Journal of Neuroscience*, *31*, 978–993. https://doi.org/10.1111/j.1460-9568.2010.07133.x

de Jonge, W. J., van der Zanden, E. P., The, F. O., Bijlsma, M. F., van Westerloo, D. J., Bennink, R. J., Berthoud, H. R., Uematsu, S., Akira, S., van den Wijngaard, R. M., & Boeckxstaens, G. E. (2005). Stimulation of the vagus nerve attenuates macrophage activation by activating the Jak2-STAT3 signaling pathway. *Nature Immunology*, *6*, 844–851. https://doi.org/10.1038/ni1229

de Lucas-Cerrillo, A. M., Maldifassi, M. C., Arnalich, F., Renart, J., Atienza, G., Serantes, R., Cruces, J., Sanchez-Pacheco, A., Andres-Mateos, E., & Montiel, C. (2011). Function of partially duplicated human alpha7 nicotinic receptor subunit CHRFAM7A gene: Potential implications for the cholinergic anti-inflammatory response. *The Journal of Biological Chemistry*, *286*, 594–606. https://doi.org/10.1074/jbc.M110.180067

Di Lascio, S., Fornasari, D., & Benfante, R. (2022). The human-restricted isoform of the alpha7 nAChR, CHRFAM7A: A double-edged sword in neurological and inflammatory disorders. *International Journal of Molecular Sciences*, *23*, 3463. https://doi.org/10.3390/ijms23073463

Fischer, H., Orr-Urtreger, A., Role, L. W., & Huck, S. (2005). Selective deletion of the α5 subunit differentially affects somatic-dendritic versus axonally targeted nicotinic ACh receptors in mouse. *The Journal of Physiology*, *563*, 119–137. https://doi.org/10.1113/jphysiol.2004.075788

Gault, J., Hopkins, J., Berger, R., Drebing, C., Logel, J., Walton, C., Short, M., Vianzon, R., Olincy, A., Ross, R. G., Adler, L. E., Freedman, R., & Leonard, S. (2003). Comparison of polymorphisms in the alpha7 nicotinic receptor gene and its partial duplication in schizophrenic and control subjects. *American Journal of Medical Genetics. Part B, Neuropsychiatric Genetics*, *123B*, 39–49. https://doi.org/10.1002/ajmg.b.20061

Gault, J., Robinson, M., Berger, R., Drebing, C., Logel, J., Hopkins, J., Moore, T., Jacobs, S., Meriwether, J., Choi, M. J., Kim, E. J., Walton, K., Buiting, K., Davis, A., Breese, C., Freedman, R., & Leonard, S. (1998). Genomic organization and partial duplication of the human alpha7 neuronal nicotinic acetylcholine receptor gene (CHRNA7). *Genomics*, *52*, 173–185. https://doi.org/10.1006/geno.1998.5363

George, A. A., Vieira, J. M., Xavier-Jackson, C., Gee, M. T., Cirrito, J. R., Bimonte-Nelson, H. A., Picciotto, M. R., Lukas, R. J., & Whiteaker, P. (2021). Implications of oligomeric amyloid-beta (oAbeta42) signaling through alpha7beta2-nicotinic

acetylcholine receptors (nAChRs) on basal forebrain cholinergic neuronal intrinsic excitability and cognitive decline. *The Journal of Neuroscience*, *41*, 555–575. https://doi.org/10.1523/JNEUROSCI.0876-20.2020

Gill, J. K., Savolainen, M., Young, G. T., Zwart, R., Sher, E., & Millar, N. S. (2011). Agonist activation of alpha7 nicotinic acetylcholine receptors via an allosteric transmembrane site. *Proceedings of the National Academy of Sciences of the United States of America*, *108*, 5867–5872. https://doi.org/10.1073/pnas.1017975108

Gillentine, M. A., & Schaaf, C. P. (2015). The human clinical phenotypes of altered CHRNA7 copy number. *Biochemical Pharmacology*, *97*, 352–362. https://doi.org/10.1016/j.bcp.2015.06.012

Gillentine, M. A., Yin, J., Bajic, A., Zhang, P., Cummock, S., Kim, J. J., & Schaaf, C. P. (2017). Functional consequences of CHRNA7 copy-number alterations in induced pluripotent stem cells and neural progenitor cells. *American Journal of Human Genetics*, *101*, 874–887. https://doi.org/10.1016/j.ajhg.2017.09.024

Ihnatovych, I., Birkaya, B., Notari, E., & Szigeti, K. (2020). iPSC-derived microglia for modeling human-specific DAMP and PAMP responses in the context of Alzheimer's disease. *International Journal of Molecular Sciences*, *21*, 9668. https://doi.org/10.3390/ijms21249668

Ihnatovych, I., Nayak, T. K., Ouf, A., Sule, N., Birkaya, B., Chaves, L., Auerbach, A., & Szigeti, K. (2019). iPSC model of CHRFAM7A effect on alpha7 nicotinic acetylcholine receptor function in the human context. *Translational Psychiatry*, *9*, 59. https://doi.org/10.1038/s41398-019-0375-z

Ihnatovych, I., Saddler, R. A., Sule, N., & Szigeti, K. (2024). Translational implications of CHRFAM7A, an elusive human-restricted fusion gene. *Molecular Psychiatry*, *29*, 1020–1032. https://doi.org/10.1038/s41380-023-02389-1

Kabbani, N., Nordman, J. C., Corgiat, B. A., Veltri, D. P., Shehu, A., Seymour, V. A., & Adams, D. J. (2013). Are nicotinic acetylcholine receptors coupled to G proteins? *BioEssays*, *35*, 1025–1034. https://doi.org/10.1002/bies.201300082

King, J. R., Nordman, J. C., Bridges, S. P., Lin, M. K., & Kabbani, N. (2015). Identification and characterization of a G protein-binding cluster in α7 nicotinic acetylcholine receptors. *J.Biol. Chem.*, *290*, 20060–20070. https://doi.org/10.1074/jbc.M115.647040

Koukouli, F., & Maskos, U. (2015). The multiple roles of the alpha7 nicotinic acetylcholine receptor in modulating glutamatergic systems in the normal and diseased nervous system. *Biochemical Pharmacology*, *97*, 378–387. https://doi.org/10.1016/j.bcp.2015.07.018

Koukouli, F., Rooy, M., Tziotis, D., Sailor, K. A., O'Neill, H. C., Levenga, J., Witte, M., Nilges, M., Changeux, J. P., Hoeffer, C. A., Stitzel, J. A., Gutkin, B. S., DiGregorio, D. A., & Maskos, U. (2017). Nicotine reverses hypofrontality in animal models of addiction and schizophrenia. *Nature Medicine*, *23*, 347–354. https://doi.org/10.1038/nm.4274

Lang, B., Pu, J., Hunter, I., Liu, M., Martin-Granados, C., Reilly, T. J., Gao, G. D., Guan, Z. L., Li, W. D., Shi, Y. Y., He, G., He, L., Stefansson, H., St Clair, D., Blackwood, D. H., McCaig, C. D., & Shen, S. (2014). Recurrent deletions of ULK4 in schizophrenia: A gene crucial for neuritogenesis and neuronal motility. *Journal of Cell Science*, *127*, 630–640. https://doi.org/10.1242/jcs.137604

Larsen, H. M., Hansen, S. K., Mikkelsen, J. D., Hyttel, P., & Stummann, T. C. (2019). Alpha7 nicotinic acetylcholine receptors and neural network synaptic transmission in human induced pluripotent stem cell-derived neurons. *Stem Cell Research*, *41*, 101642. https://doi.org/10.1016/j.scr.2019.101642

Lasala, M., Corradi, J., Bruzzone, A., Esandi, M. D. C., & Bouzat, C. (2018). A human-specific, truncated alpha7 nicotinic receptor subunit assembles with full-length alpha7 and forms functional receptors with different stoichiometries. *The Journal of Biological Chemistry*, *293*, 10707–10717. https://doi.org/10.1074/jbc.RA117.001698

Lew, A. R., Kellermayer, T. R., Sule, B. P., & Szigeti, K. (2018). Copy number variations in adult-onset neuropsychiatric diseases. *Current Genomics*, *19*, 420–430. https://doi.org/10.2174/1389202919666180330153842

Llach Pou, M., Thiberge, C., Pons, S., Maskos, U., Cloëz-Tayarani, I. (2024) *CHRFAM7A* overexpression in human iPSC-derived Interneurons dysregulates α7-nAChR surface expression and alters response to oligomeric β-amyloid peptide. bioRxiv https://doi.org/10.1101/2024.06.04.597325

Maldifassi, M. C., Martin-Sanchez, C., Atienza, G., Cedillo, J. L., Arnalich, F., Bordas, A., Zafra, F., Gimenez, C., Extremera, M., Renart, J., & Montiel, C. (2018). Interaction of the alpha7-nicotinic subunit with its human-specific duplicated dupalpha7 isoform in mammalian cells: Relevance in human inflammatory responses. *The Journal of Biological Chemistry*, *293*, 13874–13888. https://doi.org/10.1074/jbc.RA118.003443

Martin-Sanchez, C., Ales, E., Balseiro-Gomez, S., Atienza, G., Arnalich, F., Bordas, A., Cedillo, J. L., Extremera, M., Chavez-Reyes, A., & Montiel, C. (2021). The human-specific duplicated alpha7 gene inhibits the ancestral alpha7, negatively regulating nicotinic acetylcholine receptor-mediated transmitter release. *The Journal of Biological Chemistry*, *296*, 100341. https://doi.org/10.1016/j.jbc.2021.100341

Maskos, U., Molles, B. E., Pons, S., Besson, M., Guiard, B. P., Guilloux, J. P., Evrard, A., Cazala, P., Cormier, A., Mameli-Engvall, M., Dufour, N., Cloez-Tayarani, I., Bemelmans, A. P., Mallet, J., Gardier, A. M., David, V., Faure, P., Granon, S., & Changeux, J. P. (2005). Nicotine reinforcement and cognition restored by targeted expression of nicotinic receptors. *Nature*, *436*, 103–107. https://doi.org/10.1038/nature03694

Orr-Urtreger, A., Goldner, F. M., Saeki, M., Lorenzo, I., Goldberg, L., De Biasi, M., Dani, J. A., Patrick, J. W., & Beaudet, A. L. (1997). Mice deficient in the alpha7 neuronal nicotinic acetylcholine receptor lack alpha-bungarotoxin binding sites and hippocampal fast nicotinic currents. *The Journal of Neuroscience*, *17*, 9165–9171. https://doi.org/10.1523/JNEUROSCI.17-23-09165.1997

Pastor, V., & Medina, J. H. (2023). alpha7 nicotinic acetylcholine receptor in memory processing. *The European Journal of Neuroscience*, *59*, 2138–2154. https://doi.org/10.1111/ejn.15913

Piovesana, R., Salazar Intriago, M. S., Dini, L., & Tata, A. M. (2021). Cholinergic modulation of neuroinflammation: Focus on alpha7 nicotinic receptor. *International Journal of Molecular Sciences*, *22*, 4912.

Rosa, F., Dhingra, A., Uysal, B., Mendis, G. D. C., Loeffler, H., Elsen, G., Mueller, S., Schwarz, N., Castillo-Lizardo, M., Cuddy, C., Becker, F., Heutink, P., Reid, C. A., Petrou, S., Lerche, H., & Maljevic, S. (2020). In vitro differentiated human stem cell-derived neurons reproduce synaptic synchronicity arising during neurodevelopment. *Stem Cell Reports*, *15*, 22–37. https://doi.org/10.1016/j.stemcr.2020.05.015

Seddik, R., Bradaia, A., & Trouslard, J. (2003). Choline induces Ca^{2+} entry in cultured sympathetic neurones isolated from rat superior cervical ganglion. *European Journal of Pharmacology*, *471*, 165–176. https://doi.org/10.1016/S0014-2999(03)01860-0

Seguela, P., Wadiche, J., Dineley-Miller, K., Dani, J. A., & Patrick, J. W. (1993). Molecular cloning, functional properties, and distribution of rat brain α7: A nicotinic cation channel highly permeable to calcium. *The Journal of Neuroscience*, *13*, 596–604. https://doi.org/10.1523/JNEUROSCI.13-02-00596.1993

Simeone, X., Karch, R., Ciuraszkiewicz, A., Orr-Urtreger, A., Lemmens-Gruber, R., Scholze, P., & Huck, S. (2019). The role of the nAChR subunits alpha5, beta2, and beta4 on synaptic transmission in the mouse superior cervical ganglion. *Physiological Reports*, *7*, e14023. https://doi.org/10.14814/phy2.14023

Sinkus, M. L., Graw, S., Freedman, R., Ross, R. G., Lester, H. A., & Leonard, S. (2015). The human CHRNA7 and CHRFAM7A genes: A review of the genetics, regulation, and function. *Neuropharmacology*, *96*, 274–288. https://doi.org/10.1016/j.neuropharm.2015.02.006

Szigeti, K., Ihnatovych, I., Birkaya, B., Chen, Z., Ouf, A., Indurthi, D. C., Bard, J. E., Kann, J., Adams, A., Chaves, L., Sule, N., Reisch, J. S., Pavlik, V., Benedict, R. H. B., Auerbach, A., & Wilding, G. (2020). CHRFAM7A: A human specific fusion gene, accounts for the translational gap for cholinergic strategies in Alzheimer's disease. *eBioMedicine*, *59*, 102892. https://doi.org/10.1016/j.ebiom.2020.102892

Szigeti, K., Ihnatovych, I., Rosas, N., Dorn, R. P., Notari, E., Cortes Gomez, E., He, M., Maly, I., Prasad, S., Nimmer, E., Heo, Y., Fuchsova, B., Bennett, D. A., Hofmann, W. A., Pralle, A., Bae, Y., & Wang, J. (2023). Neuronal actin cytoskeleton gain of function in the human brain. *eBioMedicine*, *95*, 104725. https://doi.org/10.1016/j.ebiom.2023.104725

Wang, Y., Xiao, C., Indersmitten, T., Freedman, R., Leonard, S., & Lester, H. A. (2014). The duplicated alpha7 subunits assemble and form functional nicotinic receptors with the full-length alpha7. *The Journal of Biological Chemistry*, *289*, 26451–26463. https://doi.org/10.1074/jbc.M114.582858

Wu, J., Liu, Q., Tang, P., Mikkelsen, J. D., Shen, J., Whiteaker, P., & Yakel, J. L. (2016). Heteromeric alpha7beta2 nicotinic acetylcholine receptors in the brain. *Trends in Pharmacological Sciences*, *37*, 562–574. https://doi.org/10.1016/j.tips.2016.03.005

Zhong, C., Talmage, D. A., & Role, L. W. (2013). Nicotine elicits prolonged calcium signaling along ventral hippocampal axons. *PLoS ONE*, *8*, e82719. https://doi.org/10.1371/journal.pone.0082719

SUPPORTING INFORMATION

Additional supporting information can be found online in the Supporting Information section at the end of this article.

How to cite this article: Görgülü, I., Jagannath, V., Pons, S., Koniuszewski, F., Groszer, M., Maskos, U., Huck, S., & Scholze, P. (2024). The human-specific nicotinic receptor subunit CHRFAM7A reduces α7 receptor function in human induced pluripotent stem cells-derived and transgenic mouse neurons. *European Journal of Neuroscience*, *60*(5), 4893–4906. https://doi.org/10.1111/ejn.16474